

ELASTOGRAPHY: FROM THEORY TO CLINICAL APPLICATIONS

Elisa E. Konofagou (1), Jonathan Ophir (2), Thomas A. Krouskop (3) and Brian S. Garra (4)

(1) Focused Ultrasound Laboratory, Department of Radiology, Brigham and Women's Hospital - Harvard Medical School, Boston, MA

(2) Ultrasonics Laboratory, Department of Radiology, University of Texas Medical School, Houston, TX

(3) Department of Physical Medicine and Rehabilitation, Baylor College of Medicine, Houston, TX

(4) Department of Radiology, Fletcher Allen Medical Center, University of Vermont, Burlington, VT

INTRODUCTION

In the past decade, an important field that has emerged as complementary to ultrasonic imaging is that of Elasticity imaging. The term encompasses a variety of techniques that can depict a mechanical response or property of tissues. In ultrasound, its premise is built on two known facts: a) that significant differences between mechanical properties of several tissue components exist and b) that the information contained in the coherent scattering, or speckle, is sufficient to depict these differences following an external or internal mechanical stimulus. Figure 1 demonstrates the validity of the first fact by showing the range of elastic moduli for several different normal and pathological human breast tissues [1]. Not only is the hardness of fat different than that of glandular tissue, but, most importantly, the hardness of normal glandular tissue is different than that of tumorous tissue (benign or malignant) by up to one order of magnitude. This is also the reason why palpation has been proven an essential tool in the detection and localization of cancer.

The second observation is based on the fact that coherent echoes can be tracked while or after the tissue in question undergoes motion and/or deformation caused by a mechanical stimulus. Elastography is a technique that employs an external quasi-static compression (on the order of 0.5-1% applied strain) in order to induce strain inside the tissue scanned. Figure 2 shows the general concept behind Elastography by showing the example of an applied compression used to detect a harder lump embedded in a softer medium. The Radio-Frequency (RF) ultrasonic data before and after the applied compression are acquired and speckle tracking techniques, e.g., crosscorrelation methods, are employed in order to calculate the resulting strain [2,3]. The resulting strain image is called elastogram.

Each pixel on the elastogram denotes the estimated amount of strain, $\hat{\epsilon}$, which the tissue experienced during the applied compression, defined by

$$\hat{\epsilon} = \frac{\hat{\tau}_1 - \hat{\tau}_2}{\Delta t}, \quad (1)$$

where $\hat{\tau}_1$ and $\hat{\tau}_2$ denote the estimates of the local tissue displacements spaced apart by the window shift Δt , which is typically on the order of 0.1-0.2 mm [3,4]. In principle, an elastogram can depict the magnitude of any one of the three principal components of strain [3], but in the subsequent figures, only the axial, i.e., parallel to the beam propagation (and RF signals in Fig.2) component is shown.

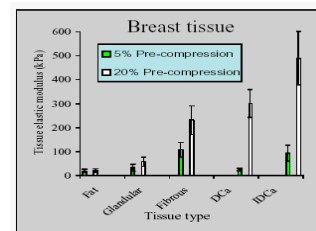


Figure 1. Elastic moduli of normal and tumorous breast tissues; DCA: ductal carcinoma, IDCa: invasive ductal carcinoma [1,4].

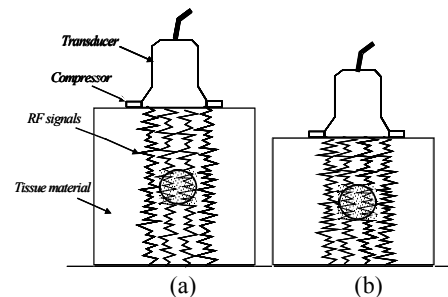


Figure 2. The principle of Elastography: The tissue is insonified a) before and b) after a small uniform compression. In the harder tissues (e.g. the circular lesion depicted) the echoes will be less distorted than in the surrounding tissues, denoting thus smaller strain.

EXAMPLES AND DISCUSSION

Figure 3 shows a typical example of a clinical application of elastography that is based on its initial premise, i.e., that of detecting stiffer nodules in tissues like the breast (Fig. 1). Both benign and malignant tumors can be differentiated from the surrounding, normal tissue. More importantly, their type could be characterized through comparison between the sonogram and the corresponding elastogram. In the case of the benign tumor, the lesion on the sonogram appears of comparable size to that of the elastogram. In the case of the malignant tumor, the opposite is true: the lesion appears larger on the elastogram. This is possibly due to the desmoplasia of the malignant tumor that results to the perilesional tissue being dragged together with the tumor while the latter is in motion; making the tumor, thus, appear larger when the strain is estimated. This is an important feature that together with the amount of strain estimated within the tumor has been shown to allow elastography to be used as a tool for cancer detection and characterization with a reliability similar to that of the PAP smear [4].

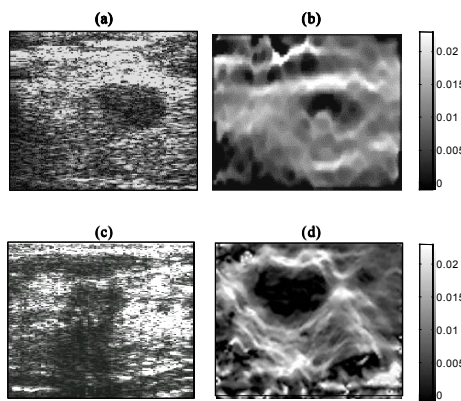


Figure 3: a) Sonogram and b) Elastogram of an in vivo benign breast tumor (fibroadenoma); c) Sonogram and d) Elastogram of an in vivo malignant breast tumor (invasive ductal carcinoma). Grayscale depicts the strain (not in %).

Except for the initial application of elastography for tumor detection, a variety of recent applications have emerged in the last few years, spanning from poroelastic property estimation [3] to High-intensity Focused Ultrasound (HIFU) lesion detection [5]. In fact, the displacement and strain parameters can also be used for the estimation of the underlying properties of the tissue in question. Those are the Poisson's ratio [3], the mobility of lesions [3] and the elastic modulus [6] to name a few. An even more significant outcome from the elastographic studies in recent years is that the image quality of the elastograms is such so as to allow depiction of tissue components within a normal organ of a certain organized structure. Such tissues include kidneys [5] and prostates (Fig. 4). In Fig. 4, the sonogram, elastogram and pathology image taken from the same image plane in the case of a normal canine prostate in vitro are shown. In this normal case, the elastogram is capable of depicting the different anatomical structures of the prostate, such as the urethra and the peripheral zones, based on their distinct mechanical response following the compression. The strain can then be related back to the underlying property or structure. For example, the peripheral zone and the verumontanum appear much stiffer than the rest of the other structures. On the other hand, the urethral crest undergoes the highest strain given the existence of the cavity and higher fluid content. Most importantly, the high contrast in strain leads to a finer definition of the tissue components in the elastogram (Fig. 4b) than in the sonogram (Fig. 4a).

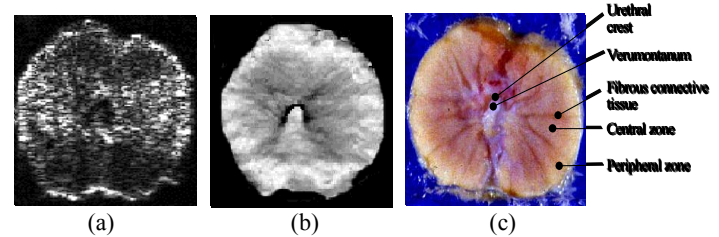


Figure 4: a) Sonogram, b) Elastogram and c) Pathology of a canine prostate in vitro. Note that, in this case, black and white denote highest and lowest strains, respectively.

Despite the fact that in its original concept, elastography employs an externally applied compression, the inherent motion or deformation of the tissues themselves can also be utilized. As a result, intravascular [7] and cardiac [8] applications of elastography have been developed. In its cardiac application, elastography has been shown capable of imaging the incremental strain that the ventricular muscle undergoes between successive sonographic frames during a cardiac cycle. Figure 5 shows such an example of a series of cardiac elastograms generated successively over the course of one cardiac cycle in a normal subject. In this case, both compressive (positive) and tensile (negative) strains were estimated. The elastograms clearly show the distribution of strain from the epicardium to the ventricular cavity and highlight a compressive-tensile strain polarity across the ventricular wall that is repeatedly reversed at different instants of the cardiac cycle. This can be shown to be consistent to the underlying fiber structure inside the muscle [8]. In conclusion, a few representative examples of the numerous applications of elastography were shown. The high quality obtained in recent years has provided unique information on several mechanical attributes in a variety of tissues that may be proven critical in the accurate detection and characterization of normal and pathological tissues.

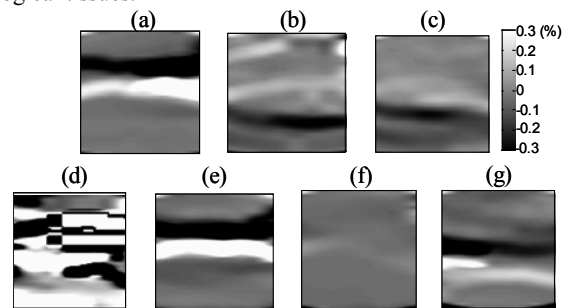


Figure 5. Cardiac elastograms in an in vivo long-axis parasternal view in a normal subject at systole ((a) 8%, b) 23%, c) 38%), d) 53% (ejection), e) 67% (fast filling), f) 75% (diastasis) and g) 97% (isovolumic contraction) of the cardiac cycle. Grayscale shows the strain (in %). The epicardium is at the top and the ventricular cavity below.

REFERENCES

1. Krouskop T.A. et al. *Ultras. Imag.* 20: 151-159, 1998.
2. Ophir J. et al., *Ultras. Imag.* 13: 111-134, 1991.
3. Konofagou E., Ph.D. Dissertation, University of Houston, 1999.
4. Garra B.S. et al., *Radiology* 202: 79-86, 1997.
5. Ophir J. et al., *J. Japan Soc. of Ultras. in Med.* 29, 2002 (in press).
6. Kallel et al. *Acous. Imag.*, 22, 267-277, 1996.
7. De Korte C., *Ultrasound Med. Biol.* 23: 735-746, 1997.
8. Konofagou E., *Ultrasound Med. Biol.* 28(4), 475-482, 2002.